COMPDYN 2013
4th ECCOMAS Thematic Conference on
Computational Methods in Structural Dynamics and Earthquake Engineering
M. Papadrakakis, V. Papadopoulos, V. Plevris (eds.)
Kos Island, Greece, 12–14 June 2013

A MACRO-ELEMENT MODEL FOR THE NONLINEAR ANALYSIS OF MASONRY MEMBERS INCLUDING SECOND ORDER EFFECTS

A. Penna[1,2] and A. Galasco[1,2]

[1]Dept. of Civil Engineering and Architecture, University of Pavia
Via Ferrata 3, I-27100 Pavia, Italy
andrea.penna@unipv.it and alessandro.galasco@unipv.it

[2]European Centre for Training and Research in Earthquake Engineering
Via Ferrata 1, I-27100 Pavia, Italy

Keywords: Masonry, Second order effects, Nonlinear analysis, Rocking, Simulation.

Abstract. *The second order effects are often neglected in the evaluation of the global seismic response of masonry buildings. Pier in-plane response is often governed by shear failure modes, particularly in case of rather squat panels and relatively high compression. Shear failure is usually associated with a limited deformation capacity which makes acceptable an approach based on the undeformed geometry of the structure. In case of structural members with a prevailing bending behaviour, the displacement capacity can be significantly increased and second order effects may no longer be negligible. Indeed, experimental tests on panels with a marked rocking behaviour show a gradual reduction of lateral strength for increasing lateral displacements, also in the absence of significant toe-crushing effects. The 2-node macro-element model implemented in the TREMURI computer program concentrates in the two extremities the coupled axial and flexural behaviour allowing for a rigorous representation of flexural cracking and toe-crushing effects. The shear response is concentrated in the central body of the element and the interaction between shear and bending-rocking behaviours is allowed by two internal degrees of freedom. The kinematic formulation of the macro-element and in particular the presence of the additional internal degrees of freedom easily allowed the introduction of P-delta effects in the nonlinear element response. Numerical results obtained with the upgraded macro-element model showed a very good agreement with experimental results. The new feature implemented in the macro-element model makes its use in the equivalent frame modelling further reliable and opens new perspectives and applications in other fields such as the analysis of rigid or quasi-rigid block systems.*

1 INTRODUCTION

Second order effects are usually neglected when dealing with modeling of the in-plane behavior of masonry walls subjected to lateral forces, since their response is normally limited to relatively small lateral displacements and deformations. For this reason, the so-called P-Δ effects are usually considered to not significantly affect the response of masonry piers. This is normally an appropriate approximation for models aiming at representing the overall behavior of masonry buildings with reasonably stiff diaphragms well connected to perimeter walls, whose behavior is governed by the in-plane strength and stiffness of walls. Nevertheless, even in some in-plane cyclic shear-compression tests (e.g. [1]) it was shown that, in case of a clear bending-rocking response, masonry piers achieving in-plane drift ratios higher than 1% show some evidence of the influence of second order effects.

On the other hand, as presented in [2], modeling strategies for representing the out-of-plane response of masonry walls often refer to limit equilibrium analysis, incorporating P-Δ effects, but usually approximating as rigid bodies the masonry portions involved in the considered damage mode (e.g. [3],[4],[5],[6]). This is also in general the approach adopted by the Italian Building Code [7] for the seismic analysis of local failure modes in existing masonry buildings with sufficient masonry quality, for which in most cases it is possible to resort to the analysis of an equivalent system consisting of a kinematic chain of rigid bodies connected in predefined points by rotational or sliding hinges (e.g. [8]). Such as approach is then suitable for the analysis of simple local failure modes, although the rigid body hypothesis and the need for preliminarily identify the position of hinges and contact points constitute its major limitations. Moreover, the study of the dynamic response of these systems is not trivial and hence the evaluation of the expected structural performance (i.e. assessment of displacement demand) is usually carried out by means of very simplified approaches [3][7].

The macro-element technique for modeling the nonlinear response of masonry panels is particularly efficient and suitable for the analysis of the seismic behavior of complex walls and buildings. With the inclusion of second order effects, this modeling approach could be extremely powerful also for assessing the structural response of masonry systems prone to local and out-of-plane failure modes when subjected to static or dynamic loadings. Accounting for P-Δ effects would also slightly improve the ability of the models in assessing the wall in-plane behavior.

2 THE MACROELEMENT MODEL

The macro-element model originally proposed by Gambarotta and Lagomarsino [8] has been further refined in the representation of flexural-rocking and shear damage modes and it is capable of fairly simulating the experimental response of in-plane cyclic tests performed on masonry piers [9]. This model is currently included in the TREMURI analysis program [10].

Based on its kinematical structure including two additional internal degrees of freedom, this 2-node macro-element model allows to describe both the shear behaviour and the coupled axial-flexural one, as well as their mutual interaction. It includes a nonlinear shear model which is derived by the macroscopic integration of a nonlinear continuum model for masonry [11]. The non linear description of the coupled relation between flexural and axial degrees of freedom allows evaluating the cracking effects on rocking motion.

Figure 1 illustrates the basic idea of the macro-element formulation. The panel can be ideally subdivided into three parts: a central body where only shear deformation can occur and

two interfaces, where the external degrees of freedom are placed, which can have relative axial displacements and rotations with respect to those of the extremities of the central body.

The two interfaces can be considered as infinitely rigid in shear and with a negligible thickness. Their axial deformations are due to distributed system of zero-length springs.

These assumptions simplify the macro-element kinematics and compatibility relations allow obtaining a reduction of the actual degrees of freedom of the model. Since the central part is considered as a rigid body with only shear deformation capability, under small displacement hypotheses, the axial displacements and rotations of the ends can be considered equal to the centroid ones (w_e, φ_e), while the transversal displacements on the central body ends must be equal to the corresponding nodal displacements (u_i, u_j).

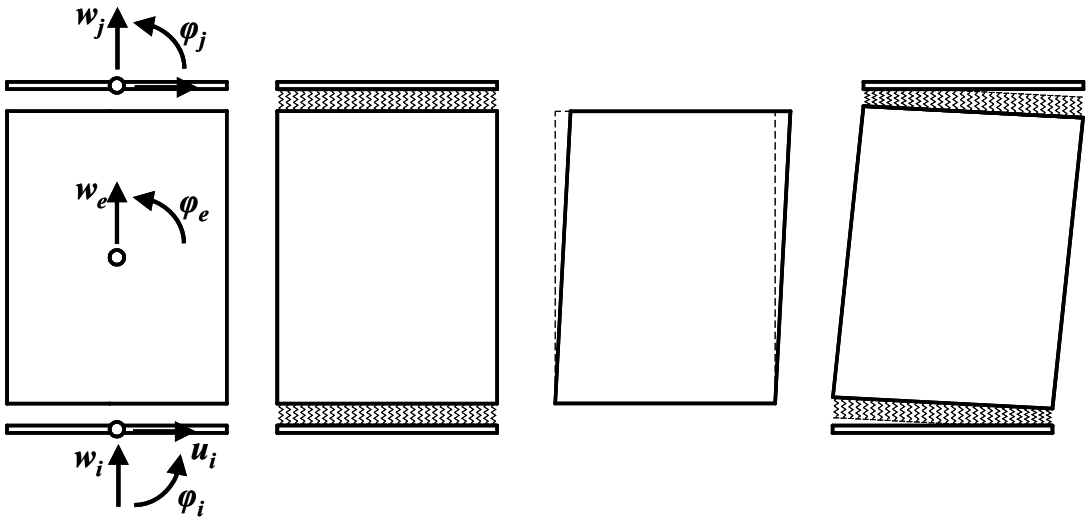

Figure 1: Kinematics of the macro-element (after [9])

Therefore the macro-element kinematics can be described by means of eight degrees of freedom, 6 nodal displacement components (u_i w_i, φ_i, u_j w_j, φ_j) and 2 internal components (w_e, φ_e).

No distributed transversal actions are considered and so the internal shear force is constant along the element axis ($V_i = V_j = V$). The shear failure mode is considered to be macroscopically representative of both the shear failure modes, diagonal cracking and sliding on bed joints, with an equivalent approach.

A no tension model has been attributed to the zero-length springs at the interfaces, with a bilinear degrading constitutive model in compression. The axial and flexural behaviour of the two extremity joints is studied separately. The static and kinematic variables involved in joint model are the element forces N and M for the considered node and the relative displacement components w and φ (Figure 2a). The relations between such variables are directly derived from the constitutive model. If the whole cross section is compressed no cracking occurs and the problem is uncoupled, with linear relations linking N and M with w and φ respectively,

$$\begin{cases} N = kltw \\ M = \dfrac{k}{12} tl^3 \varphi \end{cases} \tag{1}$$

where l is the wall length, t is the wall thickness, $k = 2E/h$ is the spring axial stiffness for surface unit, with E compressive Young modulus of masonry and h wall height (in order to reproduce the axial stiffness of the panel), w is the relative axial displacement ($w = w_i - w_e$, at

node *i* and $w = w_e - w_j$ at φ is the relative rotation ($\varphi = \varphi_i - \varphi_e$, at node I and $\varphi = \varphi_e - \varphi_j$ at node *j*).

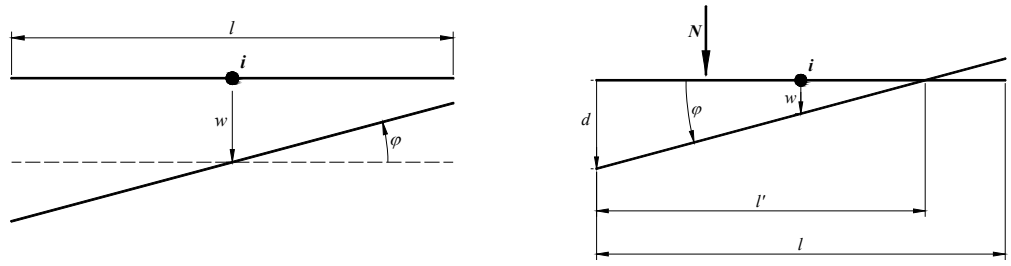

(a) (b)

Figure 2: Kinematic representation of node *i* interface in uncracked (a) and cracked (b) conditions

The cracking condition can be simply expressed in terms of kinematic variables (Figure 2b),

$$|\varphi| > \frac{2w}{l} \tag{2}$$

In cracked condition the axial force can be calculated as

$$N = -\frac{1}{2} ktl' d \,, \tag{3}$$

where *d* is the relative axial displacement at the compressed edge of the considered interface joint and *l'* is the compressed length of the cross section.

Under the small displacement hypothesis it is immediate to obtain

$$d = |\varphi| l' \,, \tag{4}$$

and therefore the expression of $|w|$

$$|w| = \left(l' - \frac{l}{2} \right) |\varphi| \,, \tag{5}$$

derived according to the similar triangles rule, can be inverted in order to obtain the length of the compressed part of the cross section, *l'*,

$$l' = \frac{w}{|\varphi|} + \frac{l}{2} = \frac{l|\varphi| + 2w}{2|\varphi|} \,, \tag{6}$$

Expression (6) can be substituted in (4) and (5) expressing the axial force as

$$N = -\frac{kt}{8|\varphi|} \left(l|\varphi| + 2w \right)^2 \,. \tag{7}$$

Imposing the rotational equilibrium around the mid point of the cross section the bending moment expression is then derived as

$$M = \frac{kt}{24} \frac{\left(l|\varphi| + w \right)}{\varphi|\varphi|} \left(l|\varphi| + 2w \right)^2 \,. \tag{8}$$

Equations (7) and (8) can be rewritten separating the elastic contribution and the corrections due to cracking.

It is evident that, in case of cracked cross section, axial force and bending moment are not uncoupled and therefore it is possible to obtain the relation between w and φ for a given axial force N,

$$w = \frac{|\varphi| l}{2} - \sqrt{\frac{-2|\varphi| N}{kt}}, \tag{9}$$

which is valid out of the uncracked range of φ values. Figure 3 shows the interaction between vertical displacement and rotation for different values of axial load.

Masonry compressive strength is usually high compared to the vertical stress due to static vertical loads. Nevertheless, from experimental tests it has been often observed that in-plane rocking mechanisms are characterized by toe crushing phenomena at the base of masonry piers, causing the limitation of the ultimate bending moment and some stiffness degradation in the further cycles. In order to include such effects into the nonlinear model, a phenomenological bilinear constitutive model with stiffness degradation has been assigned to the interface joint springs, as illustrated in [9]. These further contributions can be simply included in the nonlinear correction to N and M.

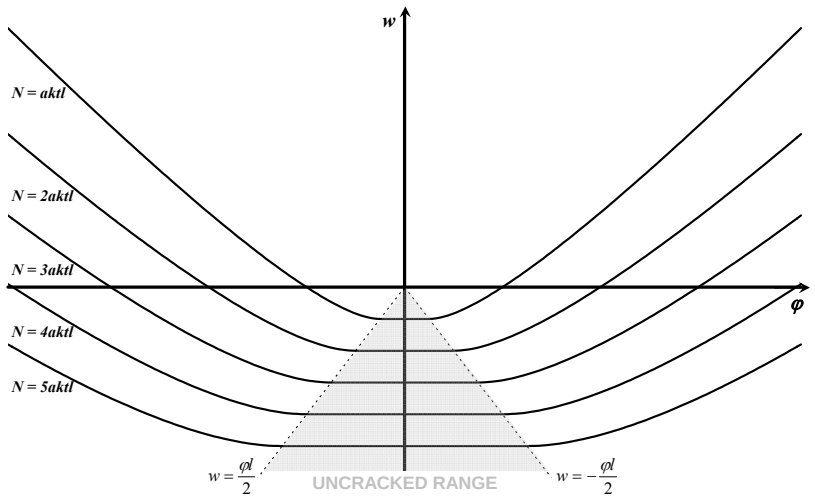

Figure 3: Interaction between w and φ for a sample wall subjected to different values of axial force (α is a constant, after [9]).

3 MACRO-ELEMENT MODEL INCLUDING SECOND ORDER EFFECTS

The constitutive model relations between the eight kinematic variables and the six nodal forces (N_i, V_i, M_i, N_i, V_j, M_j) have been derived. Internal equilibrium equations provide the forces acting on the additional degrees of freedom in the original configuration (without second order effects):

$$\begin{cases} N_e = N_j - N_i \\ M_e = M_j - M_i + Vh \end{cases}. \tag{10}$$

An easy way to include the second orders effect is to include the second order moment in the rotation equilibrium. The configuration is reported in Figure 4(b) and the relationship is given by

$$\begin{cases} N_e = N_j - N_i \\ M_e = M_j - M_i + Vh' + N_e \cdot (u_j - u_i) \end{cases} \quad (11)$$

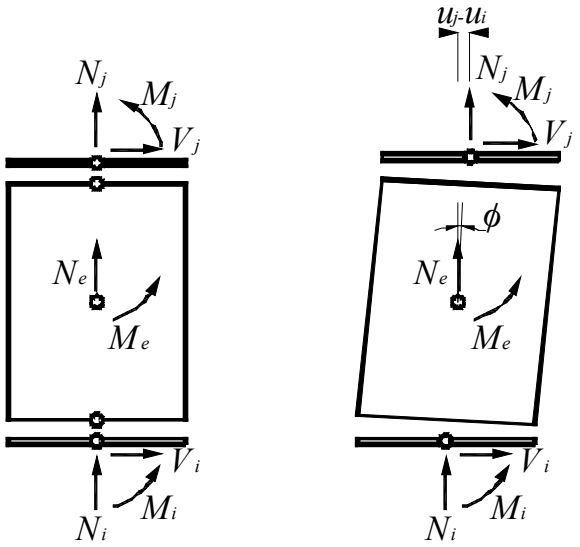

Figure 4: Equilibrium in first (a) and in second order approach (b).

Actually the arm *h'* of the moment induced by the shear force should be evaluated in the deformed shape considering both the variation in vertical displacement ($w_j - w_i$) and the rotation of the element ($h \cos \varphi$). However in a common masonry type the entity of the vertical displacement is little in comparison with the height of the element; similarly the cosine of the rotation is close to the unity so that a confusion between *h'* and *h* can be accepted.

To be consistent with the general nonlinear formulation, the second order moment can be treated as a non linear correction; according to the current notation its value is:

$$M_e^{II} = N_e \cdot (u_j - u_i) \quad (12)$$

In matrix form, subdividing the elastic and inelastic terms, the macro-element constitutive equations can then be written as

$$\begin{Bmatrix} N_i \\ V_i \\ M_i \\ N_j \\ V_j \\ M_j \\ N_e \\ M_e \end{Bmatrix} = \begin{bmatrix} klt & 0 & 0 & 0 & 0 & 0 & -klt & 0 \\ 0 & \frac{Glt}{h} & 0 & 0 & -\frac{Glt}{h} & 0 & 0 & -Glt \\ 0 & 0 & \frac{1}{12}ktl^3 & 0 & 0 & 0 & 0 & -\frac{1}{12}ktl^3 \\ 0 & 0 & 0 & klt & 0 & 0 & -klt & 0 \\ 0 & -\frac{Glt}{h} & 0 & 0 & \frac{Glt}{h} & 0 & 0 & Glt \\ 0 & 0 & 0 & 0 & 0 & \frac{1}{12}ktl^3 & 0 & -\frac{1}{12}ktl^3 \\ -klt & 0 & 0 & -klt & 0 & 0 & 2klt & 0 \\ 0 & -Glt & -\frac{1}{12}ktl^3 & 0 & Glt & -\frac{1}{12}ktl^3 & 0 & Glt + \frac{1}{6}ktl^3 \end{bmatrix} \begin{Bmatrix} w_i \\ u_i \\ \varphi_i \\ w_j \\ u_j \\ \varphi_j \\ w_e \\ \varphi_e \end{Bmatrix} - \begin{Bmatrix} N_i^* \\ V_i^* \\ M_i^* \\ N_j^* \\ V_j^* \\ M_j^* \\ 0 \\ M_e^{II} \end{Bmatrix}, \quad (13)$$

where the nonlinear correction terms identified by superscript «*» depend on cracking, toe-crushing and shear damage effects [2], while the one marked as «II» depends on the second order effects.

4 OVERTURNING BLOCK SOLUTION

The study of the overturning of a block assumed restrained only at the base (cantilever boundary conditions) represents a simple configuration to study the second order effects.

The macro-element describes a linear elastic solution up to the cracking condition according to the stiffness matrix and the boundary condition: the relationship between the horizontal top displacement u_j (here indicated only as u) and an horizontal associated forced F may be written as

$$u = \frac{Fh^3}{3EJ}, \tag{14}$$

under the hypothesis of negligible shear deformations (Euler beam solution).

At the base of the panel the equilibrium is granted by the restraint bending moment $M_i=Fh$. Usually in this phase the second order effects can be neglected. After cracking the bending moment has to satisfy the equilibrium with no tensile stress acting on the cross section (partialization). The presence of the axial vertical force N can grant a bending capacity by means of an eccentricity $e=M/N$, which, even neglecting the effect of masonry crushing (assuming an infinite compressive strength), is in any case limited to half the base of the panel.

For increasing lateral displacements (i.e. block rotations), overturning occurs and second order effects become more important contributing to the decrement of the capacity to withstand a lateral force. In Figure 5 the limit condition for which equilibrium is still possible under non-negative lateral forces is reported for the cases of only serf-weight (left) or concentrated mass at the top of the block (right). In both cases the ultimate equilibrium condition is reached when the centre of gravity of the block (or generally the application point of the vertical force) is aligned with the eccentric reaction force at the base (displacement $u=b$ for infinitely strong blocks), so that a further increase in the displacement causes an overturning of the system.

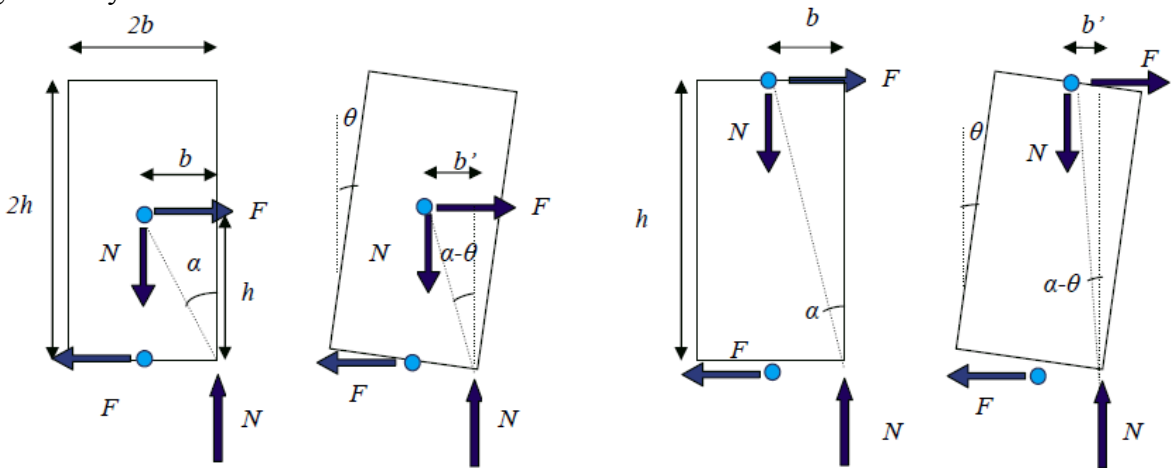

Figure 5: Limit equilibrium condition of a rigid block, subjected only to its self-weight (left) and a concentrated mass at the top (right).

With reference to the notation reported in Figure 5, the maximum lateral force that an infinitely rigid and strong block could withstand before activating overturning is given by

$$F_{\max} = \frac{Nb}{2h} \quad (15)$$

Considering the deformed configuration (block rotation), the increase of the horizontal displacement of the centre of gravity causes a reduction of the arm of the restoring moment. Assuming a rigid block and non-negative values of the angle α and θ (as reported in Figure 5) the horizontal force depends on the value of *b'* and *h'*. According to the previous consideration the value of *h* may be confused with *h'* so that only the arm of the restoring moment arm has to be evaluated:

$$F(\theta) = \frac{N \cdot b'}{2h} = \frac{N \cdot R \cdot \sin(\alpha - \theta)}{2h}, \quad (16)$$

with $R = \sqrt{b^2 + h^2}$.

For increasing values of rotation θ the lateral force decreases up to zero (for $\theta=\alpha$). In the Italian Code approach the linearization of this curve is allowed by means of the determination of $F_{\max}$ and overturning displacement [7].

4.1 Effect of elastic deformation

For non-rigid blocks, the elastic deformation is involved in the evolution of the later force capacity. As reported in Figure 6, first and second order approaches provide close results in the initial deformation phase, before cracking is reached and *u* and φ are coupled. Then the second order contribution is negative while the force due to the deformation of the interface springs increases for increasing values *u*. Hence, in the first order approach the force tends to the limit value of F_{max}, whist in the second order approach the force reaches a lower maximum value before decreasing and it is always smaller than the one of the rigid block solution (either linearized or not).

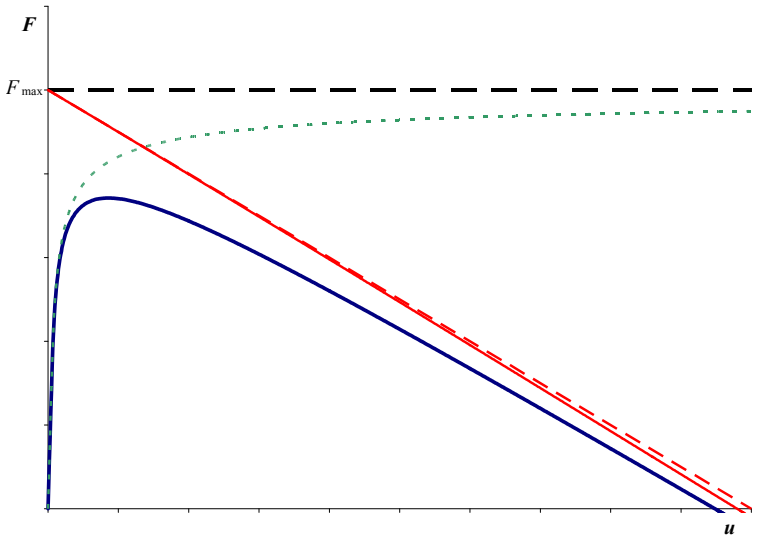

Figure 6: Comparison of force-displacement curves of a macro-element with (blue solid line) and without second order effects (green dotted line). The red curves are the rigid block solution (dashed line for the linearized solution)

In order to show the effect of the Young's modulus on the force-displacement curves, a simple numerical example is considered. It is based on a block 1.0 meter long, 2.0 meter high and 1.0 meter thick, subjected to a vertical compression of 0.5 MPa granted by a 500 kN force applied at the top (*b=0.50 m, h=2.00, t=1.00 m, N=500 kN*).

As evident fro Figure 7, for decreasing values of the Young's modulus E the value of the angle θ (assuming $\varphi \cong \theta$) corresponding to cracking condition increases, shifting the maximum value of F towards higher lateral displacements. On the other hand, the increased elastic deformation reduces the maximum value of lateral force as well as the ultimate displacement, so that decreasing E the curves are always below those of stiffer blocks.

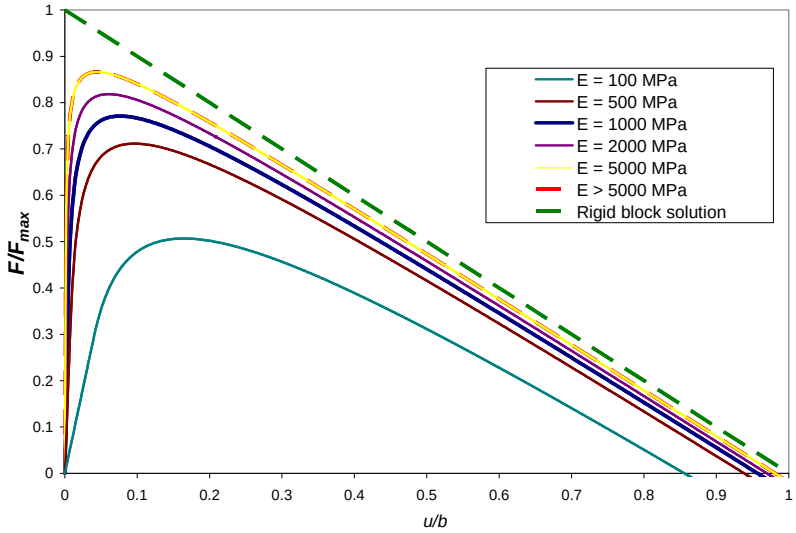

Figure 7: Force-displacement curve of a deformable macro-element for different values of the elastic modulus in compression.

4.2 Effect of limited compressive strength

The consideration of a non-infinite compression strength for the material, f_m, reduces both the value of $F_{\max}$ and the displacement corresponding to null lateral strength.

If the compressive stress is limited in its maximum value to be not greater than f_m, the maximum eccentricity of the axial force N is also limited. Assuming a complete plasticization of the compressed area of the cross section, the vertical translation equilibrium gives:

$$a = \frac{N}{2 \cdot f_m \cdot t}, \tag{17}$$

where a is the half-length of the compressed area of the cross section.

As f_m decreases, the length of the compressed area increases so that the maximum eccentricity of the axial force decreases, hence reducing the arm of the restoring moment. The reduced maximum value of F_{max} is given by

$$F'_{\max} = \frac{N(b-a)}{h} = F_{\max}\left(1 - \frac{N}{2 \cdot f_m \cdot b \cdot t}\right) \tag{18}$$

and the displacement corresponding to null lateral force decreases to

$$u'_0 = b - a = b\left(1 - \frac{N}{2 \cdot f_m \cdot b \cdot t}\right). \tag{19}$$

As shown in Figure 8, when a low value of f_m is considered, the resulting pushover curve has always lower strength than those obtained for higher values of compressive strength for corresponding displacements and it is limited by the corresponding linearized rigid body solution.

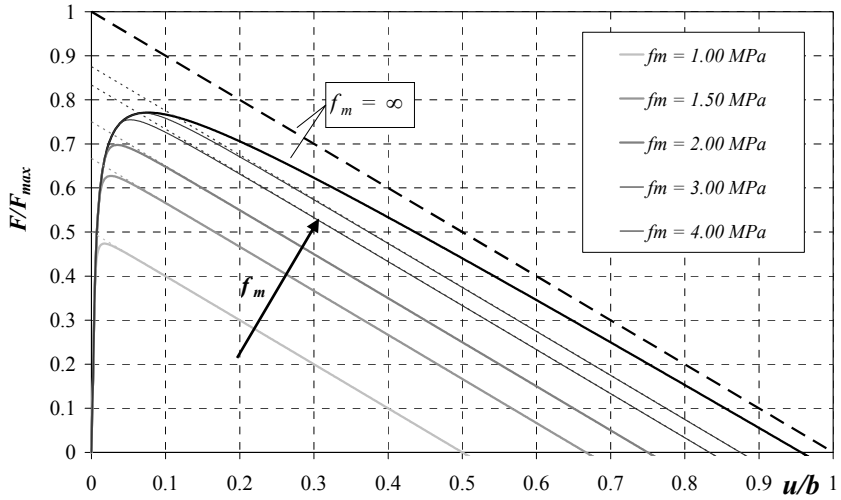

Figure 8: Comparison of force-displacement curves for a deformable macro-element obtained different values of f_m. The dashed lines correspond to the corresponding linearized rigid body solution.

5 SIMULATION OF AN IN-PLANE CYCLIC TEST ON A MASONRY WALL

The macro-element can easily reproduce the behaviour of a masonry panel during a static test (e.g. [12]); the second order correction can improve the simulation of slender panels where rocking effects involve larger displacements.

The test results reported in the following are from the testing campaign performed within the EC-FP6 ESECMaSE Project (www.esecmase.org) at the EUCENTRE Laboratory [1]. The considered specimen was a calcium-silicate masonry wall 175 mm thick, 2.5 m high and 1.25 m long, made with thin layer mortar bed- and head-joints. A vertical compression stress of 1.0 MPa was applied and several quasi-static displacement cycles were imposed to the top beam under double fixed boundary conditions.

Based on the experimental results, the macro-element parameters have been calibrated to reproduce the test results. The values are reported in the Table 1.

E [MPa]	G [MPa]	ρ [kg/m^3]	f_m [MPa]
18000	6000	1900	7.5

Table 1: Macro-element model parameters identified for the EsecMASE test CS05 [1][9]

Figure 9 shows the fair agreement between experimental and numerical results achieved considering the second order effects, which definitely improve the corresponding results from first order simulation in case of larger displacements.

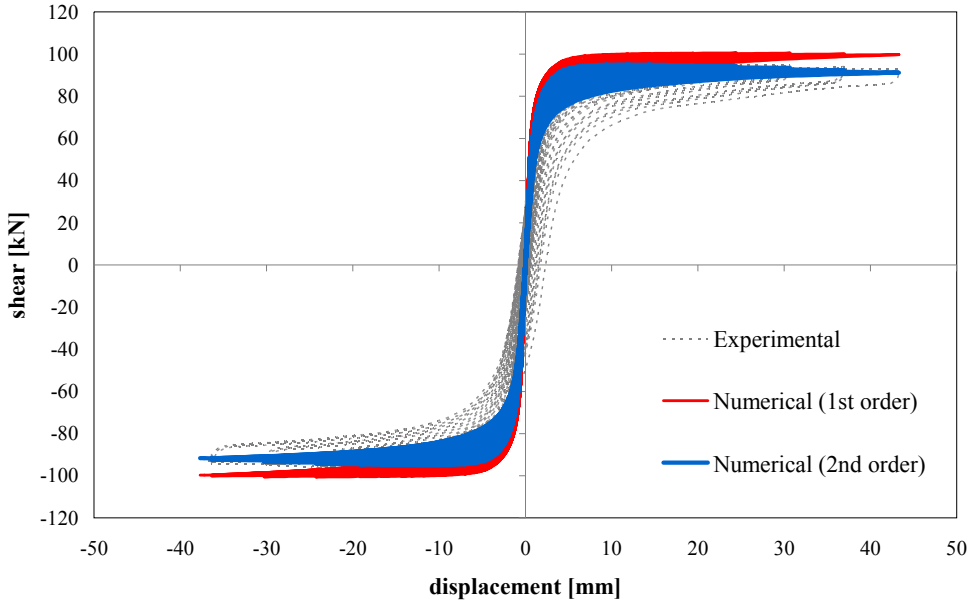

Figure 9. Comparison of the force-displacement curves obtained from in-plane cyclic test (grey dashed line) and numerical simulation with (blue) and without (red) second order effects.

6 DYNAMIC RESPONSE OF A RIGID BLOCK

The macro-element model was specifically developed to be used in dynamic simulation for seismic assessment of in-plane masonry walls [13]. The second order effect improvement can be useful to reproduce the behaviour under strong earthquake where great displacements are expected. In the following, the results obtained with the macro-element are compared to the classical theory of rocking of rigid blocks [14]. According to the Housner model [14] the free vibrations of a rigid block starting from an initial rotation around the bottom right corner (named *O*) can be expressed by the dynamic motion equation:

$$I_0 \frac{\partial^2 \vartheta}{\partial t^2} = -NR \sin(\alpha - \vartheta) \tag{20}$$

where I_0 is the moment of inertia around *O* and no energy dissipation is considered. According to the Housner's solution, assuming small angle both α and θ the equation becomes:

$$\begin{aligned} \theta'' - p^2 \vartheta &= -p^2 \alpha \\ p^2 &= NR / I_0 \end{aligned} \tag{21}$$

Assuming the initial condition $\theta = \theta_0$ *and* $\theta' = 0$ *for* $t = 0$ the analytical solution is expressed by

$$\theta = \alpha - (\alpha - \theta_0) \cosh pt \tag{22}$$

When the system falls back to the vertical position the rotation centre changes and the solution may be already working but the rotation verse of the two angle has to be inverted (a

symmetric solution around the point where θ=0). If the impact is assumed perfectly elastic no energy is dissipated due to the impact, the motion is periodic and its period is

$$T = \frac{4}{p}\cosh^{-1}\left(\frac{1}{1-\theta_0/\alpha}\right). \tag{23}$$

A very slender block, 0.2 m long, 0.1 m thick and 2.0 m high, with density equal to 1000 kg/m^3 (i.e. N = 392.4 N) is modelled using the macro-element with second order effects. According to the adopted notation b = 0.1 m, h = 1.0 m and α = 0.0997. The mass is equal to 40 kg and the moment of inertia is equal to 13.47 kg·m^2 around the centre of gravity and to 53.87 kg·m^2 around the bottom corner, respectively. The block is initially rotated imposing a horizontal translation of *0.02 m* to the center of mass, corresponding to a rotation $\theta_0 \approx 0.02$ rad, and then left oscillating in free vibrations.

As reported in Figure 10, the results are consistent with the analytical solution as shown and it can be noticed that the first order solution underestimates the period of vibration, while the second order solution provides results close to the ideal solution described by eqn. (22).

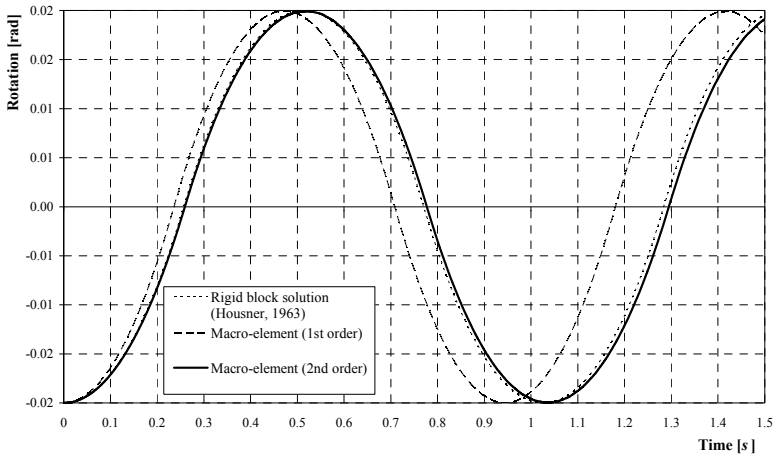

Figure 10: Rotation – time curves in analytical and numeric simulation.

In order to confirm the period prevision for different initial rotations, a comparison is reported in Figure 11. The left part of the figure show the rotation time-histories obtained for different values of relative initial rotation, while the right part of the figure illustrates the good matching between numerically obtained period values and the trend describe by eqn. (24)

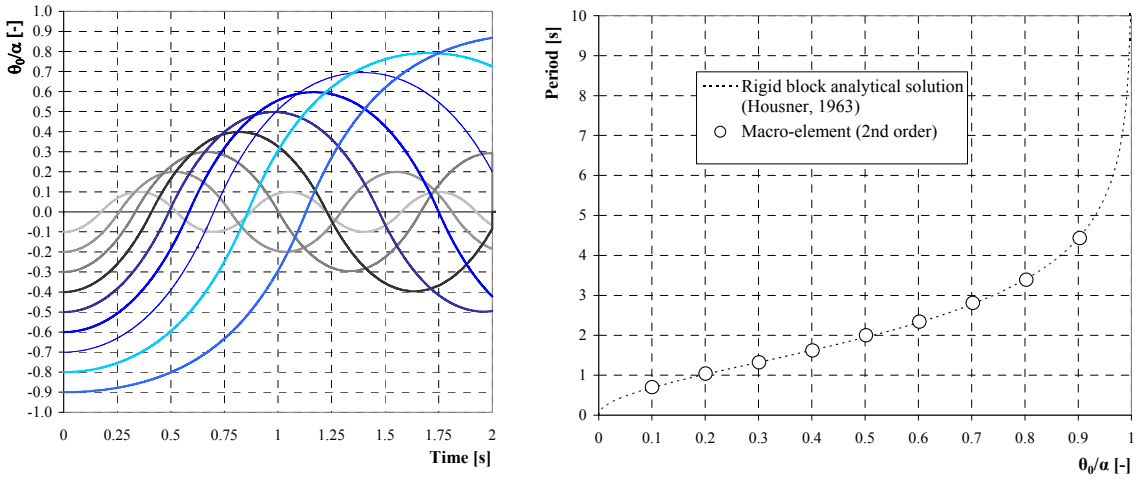

Figure 11: Left: free vibration curves of macro-elements with imposed initial rotation. Right: comparison of numerically derived vibration periods and analytical rigid block solution [14].

7 CONCLUSIONS

In this paper a modified two-dimensional macro-element model which accounts for second order effects in the analysis of blocks and/or masonry walls is presented.

The comparison of static and dynamic analysis results against experimental results and theoretical solutions confirmed that the upgraded model is able to capture the main aspects of the response of single blocks or masonry walls with rocking behaviour.

Future developments of the model will necessarily be oriented to include energy dissipation effects occurring in dynamic response.

The availability of this improved macro-element will be potentially useful for the study of out-of-plane and local failure modes occurring in masonry buildings during seismic events.

ACKNOWLEDGEMENTS

This work has been partially developed within the framework of the Eucentre Executive Project 2012-14 e3 “Seismic vulnerability of masonry buildings” and the Reluis Executive Project 2009-13 AT1-1-1 “Evaluation of the vulnerability of masonry buildings, historical centres, cultural heritage” both funded by the Italian Department of Civil Protection.

REFERENCES

[1] G. Magenes, P. Morandi, and A. Penna, In-plane cyclic tests of calcium silicate masonry walls, *Proceedings of the 14th Intl. Brick/Block Masonry Conference*, Sydney, Australia, 2008.

[2] G. Magenes, A. Penna A. Seismic design and assessment of masonry buildings in europe: recent research and code development issues, *Proceedings of the 9th Australasian Masonry Conference,* Queenstown, New Zealand, 2011.

[3] M.C. Griffith, G. Magenes, G. Melis, L. Picchi, Evaluation of out-of-plane stability of unreinforced masonry walls subjected to seismic excitation, *Journal of Earthquake Engineering*, Vol. 7, SI 1, 141-169, 2003.

[4] L. Sorrentino L., R. Masiani, M.C. Griffith, The vertical spanning strip wall as a coupled rocking rigid body assembly, *Structural Engineering and Mechanics*, 29 (4) , pp. 433-453, 2008.

[5] O. Al Shawa, G. de Felice, A. Mauro, L. Sorrentino, Out-of-plane seismic behaviour of rocking masonry walls, *Earthquake Engineering and Structural Dynamics*, 41 (5) , pp. 949-968, 2012.

[6] D. D'Ayala, Y. Shi, Modeling masonry historic buildings by multi-body dynamics, International Journal of Architectural Heritage 5 (4-5) , pp. 483-512, 2011.

[7] NTC08 Decreto Ministeriale 14 Gennaio 2008: "Norme tecniche per le costruzioni," Ministero delle Infrastrutture. S.O. n.30 alla G.U. del 4.2.2008, No. 29, 2008.

[8] L. Gambarotta and S. Lagomarsino, On the dynamic response of masonry panels, *Proc. of the National Conference "Masonry Mechanics Between Theory and Practice"*, Messina, Italy, 1996 (in Italian).

[9] A. Penna, S. Lagomarsino, A. Galasco, A nonlinear macro-element model for the seismic analysis of masonry buildings. *Earthquake Engineering and Structural Dynamics*, 2013 (in press).

[10] S. Lagomarsino, A. Penna, A. Galasco, S. Cattari, TREMURI program: an equivalent frame model for the nonlinear seismic analysis of masonry buildings. *Submitted to Engineering Structures*, 2013.

[11] L. Gambarotta, S. Lagomarsino, Damage models for the seismic response of brick masonry shear walls. Part II: the continuum model and its applications. *Earthquake Engng Struct. Dynamics* 1997; 26: 441-462.

[12] A.A. Costa, A. Penna, G. Magenes, Seismic performance of Autoclaved Aerated Concrete (AAC) masonry: from experimental testing of the in-plane capacity of walls to building response simulation, *Journal of Earthquake Engineering*, 15(1): 1-31, 2011.

[13] A. Penna, M. Rota, A. Mouyiannou, G. Magenes, Issues on the use of time-history analysis for the design and assessment of masonry structures, *Proc. 4th ECCOMAS Thematic Conference on Computational Methods in Structural Dynamics and Earthquake Engineering*, *COMPDYN 2013,* M. Papadrakakis, V. Papadopoulos, V. Plevris (eds.), Kos Island, Greece, 2013.

[14] G. W. Housner, The behaviour of inverted pendulum structures during earthquakes. *Bulletin of the Seismological Society of America*, Vol 53, No. 2, pp 403-417, 1963.